

Spring 5-13-2011

Chemistry - ACS Certification

Daniel Hinson

Western Kentucky University, daniel.hinson627@topper.wku.edu

Follow this and additional works at: http://digitalcommons.wku.edu/stu_hon_theses



Part of the [Chemistry Commons](#)

Recommended Citation

Hinson, Daniel, "Chemistry - ACS Certification" (2011). *Honors College Capstone Experience/Thesis Projects*. Paper 304.
http://digitalcommons.wku.edu/stu_hon_theses/304

This Thesis is brought to you for free and open access by TopSCHOLAR®. It has been accepted for inclusion in Honors College Capstone Experience/Thesis Projects by an authorized administrator of TopSCHOLAR®. For more information, please contact topscholar@wku.edu.

Synthetic Study of Some Organometallic Pyridazine Complexes

Presented in Fulfillment of the Requirements for
the Degree Bachelor of Science with
Honors College Graduate Distinction at Western Kentucky University

By

Daniel F. Hinson

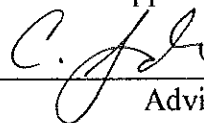
Western Kentucky University

2011

CE/T Committee:

Professor Chad Snyder, Advisor
Professor Cathleen Webb
Professor Nathan Phelps

Approved by



Advisor
Department of Chemistry

Synthetic Study of Some Organometallic Pyridazine Complexes

Presented in Fulfillment of the Requirements for
the Degree Bachelor of Science with
Honors College Graduate Distinction at Western Kentucky University

By

Daniel F. Hinson

Western Kentucky University

2011

CE/T Committee:

Professor Chad Snyder, Advisor
Professor Cathleen Webb
Professor Nathan Phelps

Approved by

Advisor
Department of Chemistry

Copyright by
Daniel F. Hinson
2011

ABSTRACT

Heterocyclic organic and organometallic compounds (e.g. polypyrrole, **Figure 1A**) and their derivatives have been of great interest for conductive polymers due to their novel properties, such as their versatile structure and ease of synthesis. In addition, these molecules have a great environmental stability compared to non-aromatic analogs (e.g. polyacetylene, **Figure 1B**). We have been interested in synthesizing organometallic pyridazyl (**Figure 1C**) complexes for polymer research.

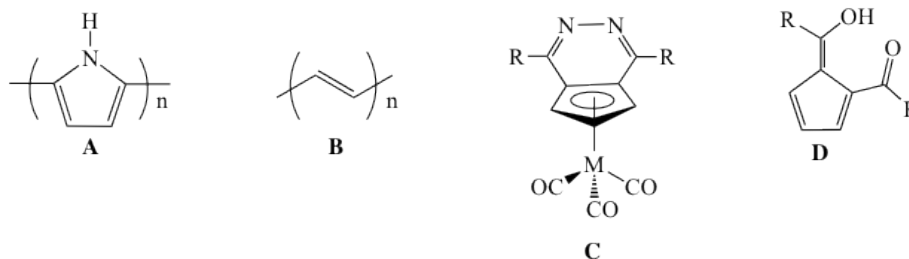


Figure 1. Structures of A–D.

Pyridazyl complexes of rhenium were synthesized in three steps beginning from 1,2-diacylcyclopentadienes (aka, fulvenes, **Figure 1D**). Synthesis, characterization and molecular structure of $[\text{Mn}(\text{CO})_3\{1,2\text{-C}_5\text{H}_3(\text{CC}_4\text{H}_3\text{ON})(\text{CC}_4\text{H}_3\text{ON})\}]$ (**4A**), $[\text{Re}(\text{CO})_3\{1,2\text{-C}_5\text{H}_3(\text{CC}_4\text{H}_3\text{ON})(\text{CC}_4\text{H}_3\text{ON})\}]$ (**4B**), and their precursors are reported here.

Keywords: Semiconductors, Organometallic, Pyridazines, Furans, Polymers, Fulvenes

ACKNOWLEDGMENTS

I would like to thank Dr. Chad Snyder for his guidance throughout my undergraduate career. He has helped me develop as a scientist both in and out of the classroom and for that I am very grateful. I would like to thank the Western Kentucky University Chemistry Department for funding me in presenting my research at the Spring 2010 and Spring 2011 American Chemical Society Convention in San Francisco and Anaheim. I would also like to thank Dr. Cathleen Webb and Dr. Nathan Phelps for serving on my thesis committee.

VITA

May 21, 1989.....Born – Nashville, Tennessee

2007.....East Robertson High School
Cross Plains, Tennessee

2010.....Poster: ACS National Meeting
San Francisco, California

2010.....Hypercube Scholar

2011.....Poster: ACS National Meeting
Anaheim, California

2011.....Outstanding Chemistry Major

PUBLICATIONS

1. Snyder, C. A.; Tice, N. C.; Maddox, J. B.; Emberton, E. D.; Vanover, E. S.; Hinson, D. F.; Jackson, D. C. Synthesis, Structure, and Electronic Study of Some Group VII Furoyl Substituted Complexes, *Journal of Organometallic Chemistry*, 2010

FIELD OF STUDY

Major Field: Chemistry w/ ACS Certification

Minor Field: Mathematics

TABLE OF CONTENTS

	<u>Page</u>
Abstract.....	ii
Acknowledgements.....	iii
Vita.....	iv
List of Figures.....	vi
Chapters:	
1. Organic Semiconductors, Pyridazines, and Furans.....	1
2. Experimental.....	10
3. Results and Discussions.....	17
4. Conclusions.....	27
References.....	28

LIST OF FIGURES

<u>Figure</u>		<u>Page</u>
Figure 1	Structures of A – D.....	ii
Figure 2	A Molecular Orbital Illustration of an insulator, semiconductor, and conductor.....	3
Figure 3	Structures of Pyridazine, Furan, and Furfural.....	9
Scheme 1	Total Synthesis of Pyridazyl Complexes.....	16
Scheme 2	Mechanism for the synthesis of fulvene, beginning with cyclopentadiene.....	18
Scheme 3	Mechanism for the synthesis of Thallium salt.....	20
Figure 4	Crystal Structure of $[\text{Mn}\{\eta^5\text{-1,2-C}_5\text{H}_3(\text{COC}_4\text{H}_3\text{O})_2\}(\text{CO})_3]$	25
Figure 5	Crystal Structure of $[\text{Re}\{\eta^5\text{-1,2-C}_5\text{H}_3(\text{COC}_4\text{H}_3\text{O})_2\}(\text{CO})_3]$	25
Table 1	Crystal Data for 3A and 3B.....	26

CHAPTER 1

ORGANIC SEMICONDUCTORS, PYRIDAZINES, AND FURANS

The world of modern electronics centers on the use of materials known as semiconductors, which are found in everything from wristwatches to calculators. Most people come into contact with semiconductors every day. Whether you're turning on the radio in your car, using your cell phone to make a call, or using your computer to check your email, semiconductors are there making your life easier. Typical semiconductors are made of inorganic conductors such as silicon. However, since the mid 1900's, scientists have been interested in a new brand of carbon-based semiconductors¹. These organic semiconductors pose multiple benefits over their inorganic analogs. Pyridazine has been a molecule of great interest in this field due to its electrochemical properties. We are working on the synthesis of a pyridazine polymer that should provide a useful semiconducting material. In order to improve the conductivity and stability of this material, we are doping this polymer with furan. This thesis discusses the synthesis and characterization of these polymers.

Conductors, Insulators, and Semiconductors

An electrical current is defined as the movement of electrons through some medium. A material's ability to conduct an electrical current varies greatly from substance to substance. Some substances are easily able to carry a current; these materials

are known as conductors. Other materials, which cannot carry a current, are known as insulators. In quantum mechanical terms, a current can only occur when electrons are able to overcome the band gap between the valence and conduction band.

Every electron has an energy associated with it. The valence band is a range of energy that electrons usually occupy. In order for there to be an electrical current, electrons must be able to move into a higher energy area known as the conduction band. In between these two bands is an energy range in which no electron can exist, known as a band gap. Conductors, such as metals, are able to easily carry a current because their conduction band is very close to or overlaps the valence band; therefore, they have almost no band gap and electrons are easily able to move into the conduction band. Insulators, however, have a very large band gap, so electrons are unable to go into the conduction band (**Figure 2**). Semiconductors have a definite band gap, but it is very small (~ 3 eV or less). In a semiconductor, electrons are able to make the jump into the band gap, but in order to do so they need a little extra energy. The electrons can obtain this required energy by absorbing energy from heat or light.

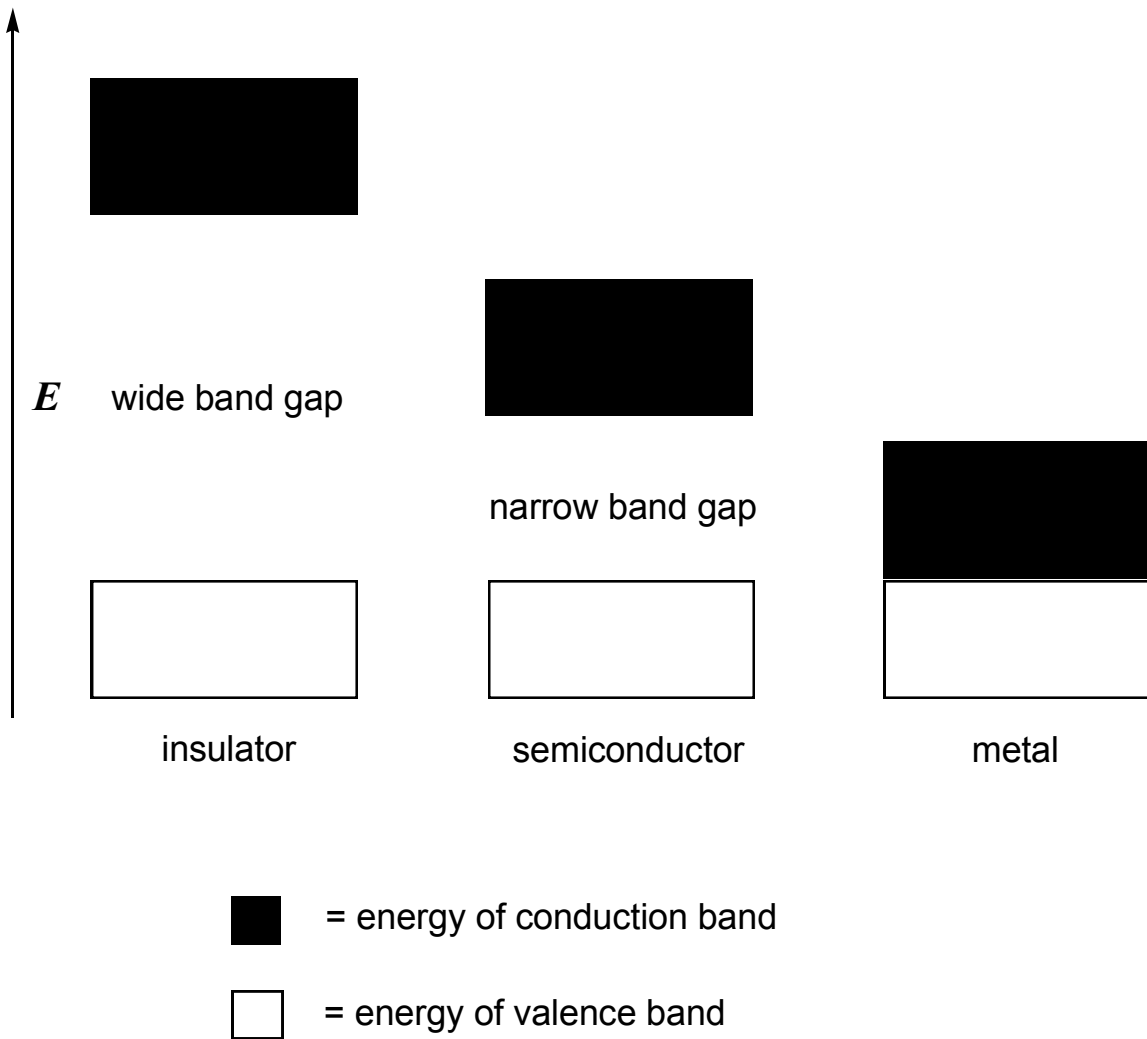


Figure 2. Molecular orbital illustration of an insulator, semiconductor, and conductor 2.

Semiconductors

Traditional semiconductors are composed of mostly silicon with a few impurities added to produce the desired conductivity. Most electrical circuits today are silicon-based. Silicon is used because it is relatively efficient, but it has many downsides. Not only can the production of silicon circuits can be expensive (the more efficient the circuit, the more expensive it is to produce), it can also be difficult. Silicon circuits require a “clean room”— a room clear of germs, dust, and debris — for production. In addition, silicon circuits need to have a rigid substrate; if they are allowed to bend they lose their conduction properties.

For the last few decades, research has gone into new semiconducting materials that consist of mostly carbon. Interest in these organic semiconductors goes back to the turn of the century. In 1906, a scientist named Pocchettino discovered a slight conductivity in solid anthracene. He released a few papers on the topic, but then interest in organic semiconductors withered away until 1941, when Szent-Gyorgi published a paper hypothesizing that electrical conductivity between molecules may play a crucial role in some biological processes (such as the nervous system). This launched a whole new interest in research of the semiconducting capabilities of organic molecules, which continues to this day ¹.

Advantages

Organic semiconductors would be able to solve most of the problems presented by silicon and other inorganic semiconductors. Organic semiconductors do not require a clean room for production. In fact, they can be produced in an ordinary laboratory. This drastically reduces the cost of production as compared to traditional inorganic

semiconductors. In addition, these materials are able to bend and still maintain their semiconducting properties. This leads to the production of flexible electronics—electronics that are able to bend, roll up, etc. and still maintain their semiconducting properties. Also, organic semiconductors are able to be dissolved into an ink or paint and still function once dried. Using this property, some companies have begun to develop printable electronics, in which you program an electronic circuit into a computer and print off a fully functioning circuit.

Silicon and other metals used to make traditional circuits must be mined for and are in limited supply. However, the sources for carbon-based semiconductors are nearly limitless. All living organisms are made of carbon and carbon dioxide is an ever increasing part of our atmosphere. Carbon could be harvested from nature and then processed in an ordinary laboratory. These semiconductors could be disposed of and/or recycled just as easily. Therefore, these semiconductors can be very sustainable and environmentally-friendly.

Applications

The study of organic semiconductors has given rise to multiple applications. However, two applications that garner the most interest are organic light-emitting diodes (OLEDs) and organic photovoltaic cells.

OLEDs

An OLED consists of an organic semiconducting material situated between two electrodes, and when a current is run through the organic material, it emits light. OLEDs have multiple advantages over standard LEDs; as mentioned earlier, OLEDs are able to be placed on a flexible material and still function, something standard LEDs are unable to

do. In addition, OLEDs are undergoing research to possibly replace liquid crystal displays (LCDs) in computer and television screens. OLEDs create their own light, whereas LED displays rely on the use of a backlight; therefore OLED screens are able to be made thinner and lighter than their LED counterparts. In addition, the ability of OLEDs to produce their own light results in a higher color contrast ratio and a deeper black level than LCD displays. OLEDs also have a faster response time and wider viewing angle.

Companies have begun to put these materials to use. The Sony XEL-1 was the world's first OLED television³. It was 11 inches wide and only 3 mm thick (these televisions can be made so thin due to their ability to function without a backlight). In 2010, Samsung introduced their revolutionary foldable 3-D television, which uses an OLED screen (as of the writing of this paper, this is still a prototype and is not available to the public)⁴.

Organic Photovoltaic Cells

Organic photovoltaic cells are solar cells which use an organic material as the semiconducting layer. The key advantages of these organic photovoltaic cells are the same as those for typical organic semiconductors given in the introduction. A major disadvantage is these materials are only able to convert light to electricity with an average of about 5% efficiency, much lower than the 10-15% efficiency produced by standard photovoltaic cells made of silicon and other inorganic materials. That single digit efficiency is hardly worth notice when compared to the more expensive devices which can reach efficiencies upwards of 40%. This gap, however, is continually closing.

In 1990, organic photovoltaic cells could barely top 1-2%; in the early 1990's a team at University of California Santa Barbara shocked scientists by making an organic photovoltaic cell with an unheard of 3% efficiency. However, in 2010 that number had risen up to over 8%. Solarmar Energy, a company highly involved in organic photovoltaic research, predicts that the efficiency of these devices could rise to above 10% within the next year or two⁵.

How They Work

Organic materials are not known for being conductive, but certain molecules have characteristics which allow them to overcome the band gap between the valence and covalent band, i.e. they allow electrons to move. Typically, organic semiconductors function as either charge-transfer complexes or conductive polymers. A charge-transfer complex is a device in which electrons are transferred between two molecules or two parts of a large molecule. I, however, am focused on conductive polymers.

A polymer is a long chain consisting of only one or two different types of molecules in a regularly repeating pattern. Common polymers, such as plastic or wood, are typically insulators. Most polymers have a large band gap, thus electrons are unable to move into the conduction band. Some polymers, however, are able to carry a current through a conjugated pi-electron cloud. This conjugated system causes a great delocalization of electrons, which allows electrons to move freely between atoms within a molecule and between molecules within the polymer. This free movement of electrons allows for the polymer to carry a current.

Pyridazines and Furans

Pyridazines have been a molecule of great interest in the field of organic semiconductors. Their planar structure and conjugated pi-electron system results in pyridazine polymers offering little hindrance to the flow of electrons. Furans have also shown to be useful in semiconducting materials. In addition to also having a conjugated π -electron system, furans have been shown to be surprisingly inert to air and water. Therefore, doping a pyridazine polymer with furan should increase the conductivity and stability of the material. Another great advantage of furans is that they can easily be derived from natural sources. For example, every year the industrial depolymerization of cellulose produces about 300,000 tons of furfural, which is a furan-based molecule (**Figure 3**)⁶. Furfural could easily be harvested, converted to furan, and used in the synthesis of these polymers.

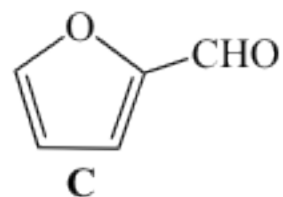
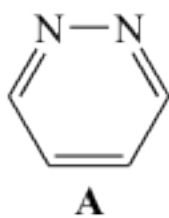


Figure 3. Structures of Pyridazine (**A**), Furan (**B**), and Furfural (**C**).

CHAPTER 2

EXPERIMENTAL

All reactions were carried out using standard Schlenk techniques under a nitrogen atmosphere unless otherwise noted. NMR solvents acetone- d_6 and $CDCl_3$ (Aldrich) were used without further purification. n BuLi, dicyclopentadiene, ethyl ether, THF, benzene (Aldrich), thallium (I) ethoxide, $[MnBr(CO)_5]$, and $[ReBr(CO)_5]$ (Strem) were used without further purification. Fulvene 1,2- $C_5H_3(COC_4H_3O)(COHC_4H_3O)$ (**1**) was prepared according to the literature methods [20]. Ethyl ether was dried over sodium benzophenone ketyl.

1H and ^{13}C NMR spectra were recorded on a JEOL-500 MHz NMR spectrometer at ca. 22 °C and were referenced to residual solvent peaks. All ^{13}C NMR spectra were listed as decoupled. Infrared spectra were recorded on Spectrum One FT-IR Spectrometer. Electron ionization (EI) mass spectra were recorded at 70 eV on a Thermo Finnigan PolarisQ (quadrupole ion trap) at the University of Kentucky Mass Spectrometry Facility. Melting points were taken on a standard Mel-Temp apparatus. X-ray diffraction data were collected at 90 K on a Nonius KappaCCD diffractometer at the University of Kentucky X-Ray Crystallographic Laboratories. Elemental analyses were performed at Western Kentucky University's Advanced Materials Institute and Atlantic Microlabs, Inc. in Norcross, GA.

Synthesis of 1,2-C₅H₃(COC₄H₃O)(COHC₄H₃O) (1)

Modified from a procedure reported by Snyder and Tice ⁷, freshly cracked cyclopentadiene (6.28 mL, 5.02 g, 76.2 mmol) in ethyl ether (20 mL) was added dropwise to a cooled solution (0 °C) of n-butyllithium (32.4 mL of 2.50 M, 46.8 g, 81.0 mmol) in ethyl ether (80 mL). A white precipitate of cyclopentadienyllithium was formed immediately. The suspension was stirred for 15 minutes and 2-furoyl chloride (5.05 mL, 6.69 g, 51.3 mmol) in ethyl ether (20 mL) was added dropwise. A bright orange color formed immediately. The solution was stirred for 45 minutes at room temperature. The reaction mixture was hydrolyzed with dilute (3%) acetic acid (100 mL). The organic layer was separated, and the aqueous layer was extracted twice more with ethyl ether (2 x 10 mL). The combined ethyl ether extracts were dried (MgSO₄) and removed under reduced pressure to leave an orange-red semi-solid. The semi-solid was eluted through a silica plug (benzene) and the only the yellow-orange band was collected. The organic solution was removed under reduced pressure to leave an orange-red solid. The solid was triturated with cold hexane (2 x 10 mL) to leave a bright orange solid (3.13 g, 12.3 mmol, 48.1%). **Mp:** 109–110 °C. **¹H NMR (500 MHz, CDCl₃, ppm):** δ 6.07 (t, 1H, ³J = 4 Hz, CHCHCH), 6.62 (dd, 1H, ³J_{AB} = 3.5 Hz, ³J_{AC} = 1.7 Hz CHCHCHO), 7.40 (d, 1H, ³J_{BC} = 3.5 Hz, CHCHCHO), 7.72 (d, 1H, ³J_{AB} = 1.7 Hz, CHCHCHO), 8.15 (d, 1H, ³J = 4 Hz, CHCHCH), 19.50 (br s, 1H, OH). **¹³C NMR (125 MHz, CDCl₃, ppm):** δ 83.8 (CHCCO), 112.5 (CHCHCH), 119.8 (CHCHCH), 123.5 (CCO), 124.1, 139.3, 146.9 (Fr), 152.0 (OCCO), 169.3 (CO). **IR (KBr, cm⁻¹):** 1530, 1565 (COC₄H₃O), 3076, 3115, 3134, 3143 (C–H). **MS:** *m/z* 254 (M⁺), 186 (M⁺ – C₄H₄O), 119 (M⁺ – 2C₄H₄O). Anal. Calcd. for C₁₅H₁₀O₂: C, 70.86; H, 3.96. Found: C, 71.47; H, 4.65.

Synthesis of [Tl{1,2-C₅H₃(COC₄H₃O)₂}] (2)

Thallium (I) ethoxide was added to a solution of 1,2-C₅H₃(COC₄H₃O)(COHC₄H₃O) (**1**, 1.15 g, 3.93 mmol) in THF (25 mL). An orange precipitate formed after 5 minutes. The solution was stirred for 3 hours at 22°C. The precipitate was filtered and washed with cold hexane (3 x 10 mL) providing [Tl{1,2-C₅H₃(COC₄H₃O)₂}] (**2**, 60.4%, 1.25 g, 1.93 mmol) as a yellow solid. **dec.** 136–150 °C. **¹H NMR (500 MHz, DMSO-d₆, ppm):** δ 5.68 (t, 1H, ³J = 3.4 Hz, CHCHCH), 6.45–6.47 (m, 4H, CHCHCHO), 6.79 (d, 1H, ³J = 3.4 Hz, CHCHCH), 7.65 (d, 2H, ³J = 1.7 Hz, CHCHCHO). **¹³C NMR (125 MHz, DMSO-d₆, ppm):** δ 111.0 (CHCHCH), 111.7 (CHCHCH), 115.3 (CCO), 122.6, 125.3, 144.7, 155.9 (Fr), 177.1 (CO). **IR (KBr, cm⁻¹):** 1572, 1537 (CO), 3112 (CH). **MS(EI-pos):** m/z 458 (M⁺). Anal. Calcd. for C₁₈H₉O₇Tl: C, 39.37; H, 1.98. Found: C, 37.29; H, 1.88.

Synthesis of [Mn{η⁵-1,2-C₅H₃(COC₄H₃O)₂}(CO)₃] (3A)

To a solution of [Tl{1,2-C₅H₃(COC₄H₃O)₂}] (**2**, 480 mg, 1.14 mmol) in dry benzene (30 mL) was added [MnBr(CO)₅] (310 mg, 1.13 mmol). The solution was allowed to reflux for 5 hours. The reaction mixture was filtered through a Celite plug using benzene. The solvent was removed under reduced pressure to leave an orange-yellow solid (**3A**, 60.7%, 250 mg, 0.617 mmol). **Mp.** 148–152 °C. **¹H NMR (500 MHz, CDCl₃, ppm):** δ 5.29 (t, 1H, ³J = 2.5 Hz, CHCHCH), 5.61 (d, 1H, ³J = 2.5 Hz, CHCHCH), 7.23–7.61 (m, 6H, CHCHCHO). **¹³C NMR (125 MHz, CDCl₃, ppm):** δ 88.3 (CHCHCH), 112.9 (CHCHCH), 118.9 (CCO), 123.5, 126.1, 131.2, 136.6 (Fr), 194.2 (CO), 211.8 (MnCO). **IR (KBr, cm⁻¹):** 3138 (CH), 2021, 1929 (MnCO), 1628 (CO).

MS: m/z 393 ($M^+ + 1$), 157 ($M^+ - C_{15}H_9O_4$). Anal. Calcd. for $C_{18}H_9O_7Mn$: C, 55.10; H, 2.30. Found: C, 55.70; H, 2.46.

Synthesis of $[Re\{\eta^5-1,2-C_5H_3(COC_4H_3O)_2\}(CO)_3]$ (**3B**)

To a solution of $[Ti\{1,2-C_5H_3(COC_4H_3O)_2\}]$ (**2**, 482 mg, 1.05 mmol) in dry benzene (30 mL) was added $[ReBr(CO)_5]$ (473 mg, 1.16 mmol). The solution was allowed to reflux for 5 hours. The solution was filtered through a Celite plug using benzene. The solvent was removed under reduced pressure to leave a red semi-solid. The semi-solid was triturated with pentane (2 x 5 mL) to provide a red powder (**3B**, 65.7%, 330 mg, 0.693 mmol). **Mp.** 82–86 °C. **1H NMR (500 MHz, $CDCl_3$, ppm):** δ 5.42 (t, 1H, $^3J = 2.9$ Hz, CHCHCH), 6.11 (d, 1H, $^3J = 2.9$ Hz, CHCHCH), 7.25–7.52 (m, 6H, CHCHCHO). **^{13}C NMR (125 MHz, $CDCl_3$, ppm):** δ 82.2 (CHCHCH), 89.6 (CHCHCH), 102.9 (CCO), 128.3, 146.8, 157.9 (Fr), 175.3 (CO), 191.4 (ReCO). **IR (KBr, cm^{-1}):** 3136 (CH), 2030, 1932 (ReCO), 1645 (CO). **MS:** m/z 524 ($M^+ + 1$), 288 ($M^+ - C_{15}H_9O_4$). Anal. Calcd. for $C_{18}H_9O_7Re$: C, 41.30; H, 1.72. Found: C, 38.78; H, 1.88.

Synthesis of $[Mn(CO)_3-\eta^5-1,2-C_5H_3(CC_4H_3ON)(CC_4H_3ON)]$ (**4A**)

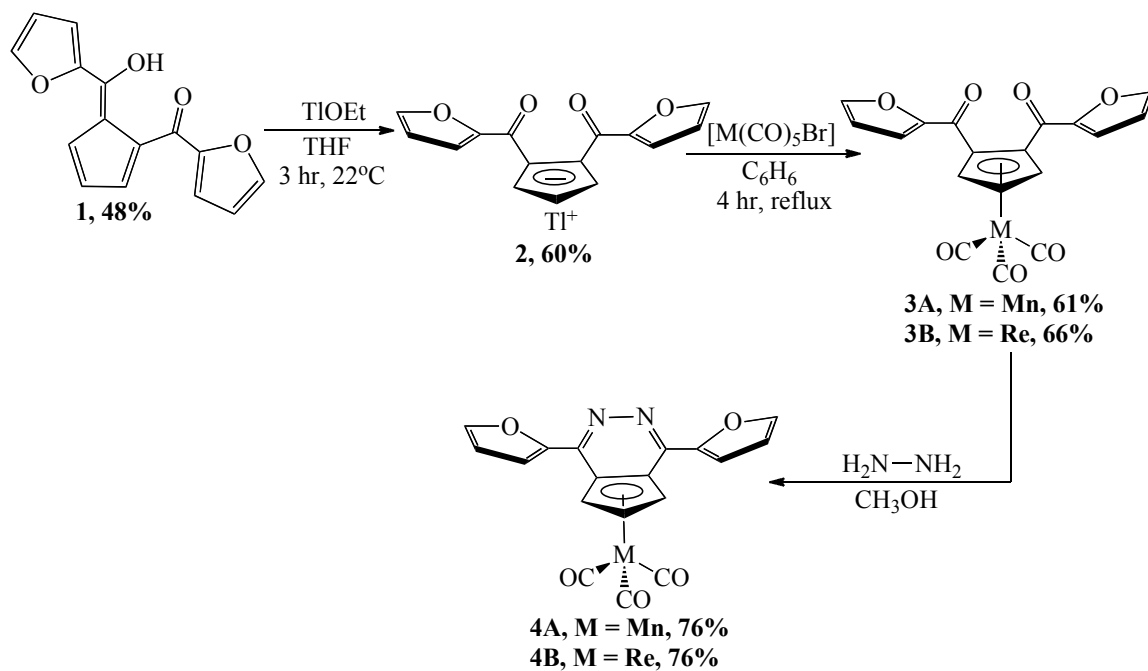
To a 20 mL round-bottom flask, $[Mn\{\eta^5-1,2-C_5H_3(COC_4H_3O)_2\}(CO)_3]$ (**3A**, 250 mg, 0.255 mmol) was dissolved in 10 mL of methanol. An excess of hydrazine hydrate (1.00 mL, 1.03 g, 20.6 mmol) was then added to the solution. The solution was stirred 24 hours at room temperature. To the reaction mixture, water (20 mL) was added and a red precipitate formed immediately. The aqueous suspension was washed with ethyl ether (3 x 5 mL) and the organic layers were collected, dried ($MgSO_4$), and filtered. The volatiles were removed *in vacuo* and the crude product was triturated with cold hexane to give

[Mn(CO)₃-η⁵-1,2-C₅H₃(CC₄H₃ON)(CC₄H₃ON)] (4A, 188 mg, 0.0644 mmol, 75.6%) as a red-orange powder. **M.p.** 60.0–64.5°C. **¹H NMR (500 MHz, acetone-d₆, ppm):** δ 5.78 (br s, 1H, CHCHCH), 6.15 (br s, 2H, CHCHCH), 6.76 (m, 2H, Fr), 7.31–8.00 (m, 4H, Fr). **¹H NMR (500 MHz, CDCl₃, ppm):** δ 5.39 (br s, 1H, CHCHCH), 5.95 (br s, 2H, CHCHCH), 6.68 (br s, 2H, Fr), 7.33–7.78 (m, 4H, Fr). **¹³C NMR (125 MHz, acetone-d₆, ppm):** δ 108.0 (CHCHCH), 112.5 (CHCHCH), 112.8 (CCN), 125.3, 132.4, 146.3, 147.7 (Fr), 151.5 (CCN), 222.5 (MnCO). **¹³C NMR (125 MHz, CDCl₃, ppm):** δ 108.4 (CHCHCH), 112.5 (CHCHCH), 112.9 (CCN), 127.3, 127.4, 133.3, 144.3 (Fr), 151.5 (CCN), 222.3 (MnCO). **IR (KBr, cm⁻¹):** 1607 (CN), 1941, 2029 (MnCO), 3060 (C–H). **MS:** *m/z* 250 (M⁺–Mn(CO)₃), 138 (M⁺–C₁₅H₉O₂N₂). Anal. Calcd. for C₁₈H₉O₅N₂Mn: C, 55.67; H, 2.32; N, 7.22. Found: C, 59.49; H, 3.13; N, 7.93.

Synthesis of [Re(CO)₃-η⁵-1,2-C₅H₃(CC₄H₃ON)(CC₄H₃ON)] (4B)

To a 50 mL round-bottom flask, [Re{η⁵-1,2-C₅H₃(COC₄H₃O)₂}(CO)₃] (3B, 200 mg, 0.382 mmol) was dissolved in 30 mL of methanol. An excess of hydrazine hydrate (1.00 mL, 1.03 g, 20.6 mmol) was then added to the solution. The solution was stirred 24 hours at room temperature. To the reaction, water (5 mL) was added and the aqueous suspension was washed with ethyl ether (3 x 2 mL) and the organic layers were collected, dried (MgSO₄), and filtered. The volatiles were removed *in vacuo* and the crude product was triturated with cold hexane to give [Re(CO)₃-η⁵-1,2-C₅H₃(CC₄H₃ON)(CC₄H₃ON)] (4B, 151.0 mg, 0.290 mmol, 76%) as a red solid. **M.p.** 125–130 °C. **¹H NMR (500 MHz, CDCl₃, ppm):** δ 7.44 (t, 1H, ³J = 7.45 Hz, CHCHCH), 7.59 (d, 2H, ³J = 7.45, CHCHCH), 7.25–7.76 (m, 6H, CHCHCHO). **¹³C NMR (125 MHz, CDCl₃, ppm):** δ 108.5 (CHCHCH), 110.0 (CHCHCH), 117.5 (CCN), 127.2, 128.8, 141.9, 144.6 (Fr),

150.9 (CCN), 221.6 (ReCO). **IR (KBr, cm^{-1}):** 1604 (CN), 1890, 2004 (ReCO), 3056 (C–H). **MS:** m/z 250 ($\text{M}^+ - \text{Re}(\text{CO})_3$). Anal. Calcd. for $\text{C}_{18}\text{H}_9\text{O}_5\text{N}_2\text{Re}$: C, 41.61; H, 1.73. Found: C, 38.73; H, 2.32.



Scheme 1. Total synthesis of pyridazyl complexes **4A–B**.⁸

CHAPTER 3

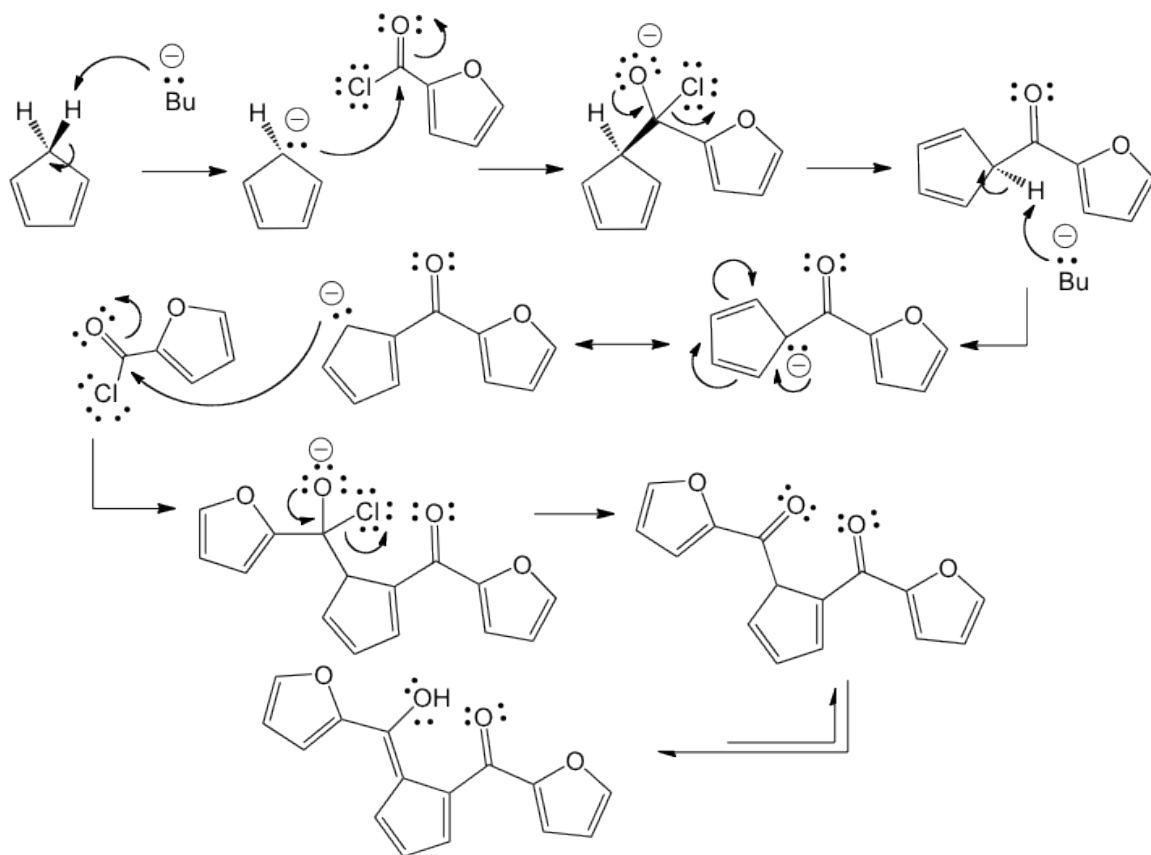
RESULTS AND DISCUSSION

Synthesis of 1,2-C₅H₃(COC₄H₃O)(COHC₄H₃O) (1)

In the first step of this reaction, dicyclopentadiene undergoes a retro Diels-Alder reaction to produce two molecules of cyclopentadiene. Cyclopentadiene was then added to a solution of n-butyl lithium, where it loses a proton to produce cyclopentadienyllithium. 2-Furoyl chloride was then added dropwise, where a 1,2 acid chloride addition occurs. We performed an aqueous workup with dilute acetic acid, followed by an extraction with ethyl ether. After drying with magnesium sulfate and removing the ether, we were left with a yellow-orange powder.

Spectroscopy of 1,2-C₅H₃(COC₄H₃O)(COHC₄H₃O) (1)

In the ¹H NMR spectrum, the furoyl protons can be seen as a doublet of doublets at 6.62 ppm (*CHCHCHO*), a doublet at 7.40 ppm (*CHCHCHO*), and a doublet at 7.72 ppm (*CHCHCHO*). The protons from the cyclopentadiene ring are observed as a doublet at 8.15 ppm (*CHCHCH*) and a triplet at 6.07 ppm (*CHCHCH*). In the ¹³C NMR spectrum, the cyclopentadiene carbons appeared at 112.5 (*CHCHCH*) and 119.8 ppm (*CHCHCH*), and the carbonyl carbon appeared at 169.3 ppm (*CO*). The carbonyl groups appeared in the IR spectrum at 1530 and 1565 cm⁻¹, which have been shifted downfield due to electron delocalization. The C—H stretches all appeared around 3100 cm⁻¹.



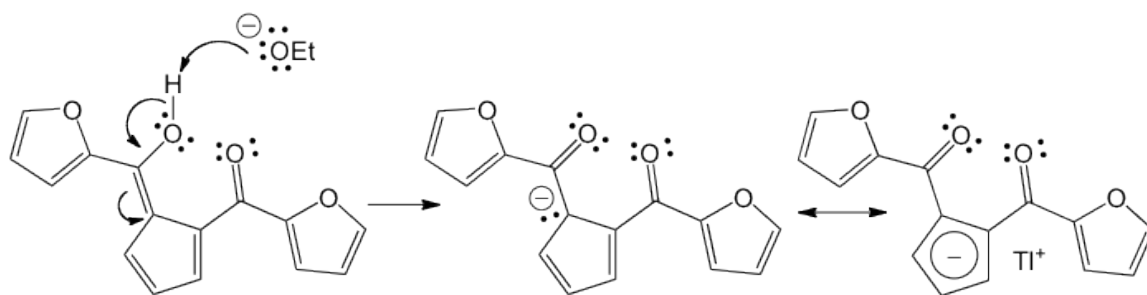
Scheme 2. Mechanism for the synthesis of fulvene, beginning with cyclopentadiene.

Synthesis of [Tl{1,2-C₅H₃(COC₄H₃O)₂}] (2)

Thallium ethoxide was added to a solution of 1,2-C₅H₃(COC₄H₃O)(COHC₄H₃O) (**1**) in THF, where it formed an orange precipitate. The thallium ethoxide reduced the hydroxyl group in molecule 1 to produce [Tl{1,2-C₅H₃(COC₄H₃O)₂}] (**2**). After stirring for three hours, the precipitate was filtered and washed with cold hexane. We were then left with a yellow powder.

Spectroscopy of [Tl{1,2-C₅H₃(COC₄H₃O)₂}] (2)

In the ¹H NMR spectrum, the cyclopentadiene protons appeared as a doublet at 6.79 ppm (*CHCHCH*) and a triplet at 5.68 ppm (*CHCHCH*). One of the furoyl protons appeared as a doublet at 7.65 ppm (*CHCHCHO*) and the others appeared in the 6.45-6.47 ppm range (*CHCHCHO*). The ¹³C NMR showed a downfield peak at 177.1 ppm for the carbonyl carbon (*CO*). The cyclopentadiene carbons appeared at 111.0 ppm (*CHCHCH*) and 111.7 ppm (*CHCHCH*), and the furoyl carbons appeared at 122.6, 125.3, 144.7, and 155.9 ppm. The IR showed a peak at 1572 and 1537 cm⁻¹ for the C=O stretch and a peak at 3112 cm⁻¹ for the C—H stretch.



Scheme 3. Mechanism for the synthesis of Thallium salt.

Synthesis of $[M\{\eta^5-1,2-C_5H_3(COC_4H_3O)_2\}(CO)_3]$ (**3A** and **3B**)

[Manganese/Rhenium] pentacarbonyl bromide was added to a solution of $[Tl\{1,2-C_5H_3(COC_4H_3O)_2\}]$ (**2**) in dry benzene. A transmetallation reaction took place, in which the thallium cation was replaced with $[M(CO)_3]$ to form $[M\{\eta^5-1,2-C_5H_3(COC_4H_3O)_2\}(CO)_3]$ (**3A/B**). After allowing to reflux for 5 hours, the solution was filtered through a Celite plug with benzene. After removing the solvent, we were left with a red semisolid which was triturated with pentane to produce a red powder. Proof that this reaction had taken place included the production of thallium bromide as a byproduct.

Spectroscopy of $[Mn\{\eta^5-1,2-C_5H_3(COC_4H_3O)_2\}(CO)_3]$ (**3A**)

In the 1H NMR spectrum, there was a doublet and a triplet at 5.61 ppm (*CHCHCH*) and 5.29 ppm (*CHCHCH*), respectively, corresponding to the cyclopentadiene protons. The furoyl protons appeared in the range of 7.23-7.61 ppm (*CHCHCHO*). The ^{13}C NMR spectrum showed peaks at 88.3 ppm (*CHCHCH*) and 112.9 ppm (*CHCHCH*) corresponding to the cyclopentadiene carbons. The carbonyl carbon (*CO*) appeared at 194.2 ppm and the carbon complexed with the manganese appeared at 211.8 ppm. The IR spectrum showed a peak at 3138 cm^{-1} for the C—H stretch, the MnCO stretch appeared at 2021 and 1929 cm^{-1} , and there was a peak at 1628 cm^{-1} for the C=O stretch. This carbonyl stretch is greatly shifted downfield due to the delocalization caused by the metal complex.

Spectroscopy of $[Re\{\eta^5-1,2-C_5H_3(COC_4H_3O)_2\}(CO)_3]$ (**3B**)

In the 1H NMR spectrum, the protons on the cyclopentadiene ring appeared as a doublet at 6.11 ppm (*CHCHCH*) and a triplet at 5.42 ppm (*CHCHCH*), and the furoyl protons appeared in the 7.25-7.52 ppm range (*CHCHCHO*). The ^{13}C NMR showed a

downfield peak at 175.3 ppm for the carbonyl carbon (CO) and a peak at 191.4 ppm for the carbon attached to the rhenium (ReCO). The cyclopentadiene carbons appeared at 82.2 ppm (CHCHCH) and 89.6 ppm (CHCHCH). The IR spectrum showed a peak at 3136 cm⁻¹ for the C—H stretch, a peak at 2030 and 1932 cm⁻¹ for the ReCO stretch, and one at 1645 cm⁻¹ for the C=O stretch, which is shifted downfield in the same way that 3B was.

Synthesis of [M(CO)₃- η⁵-1,2-C₅H₃(CC₄H₃ON)(CC₄H₃ON) }] (4A and 4B)

An excess of hydrazine hydrate was added to a solution of [M{η⁵-1,2-C₅H₃(COC₄H₃O)₂}(CO)₃] (**3A/B**) in methanol. The hydrazine closed the fulvene ring into a pyridazine ring to form [M(CO)₃- η⁵-1,2-C₅H₃(CC₄H₃ON)(CC₄H₃ON) }] (**4A/B**). The solution was allowed to stir for 24 hours, and the reaction was then quenched with water. The product was extracted using ethyl ether and purified through a silica plug. The resulting red semi-solid was triturated with cold hexane to yield a red solid.

Spectroscopy of [Mn(CO)₃- η⁵-1,2-C₅H₃(CC₄H₃ON)(CC₄H₃ON) }] (4A)

In the ¹H NMR spectrum (using acetone), the cyclopentadiene protons appeared at 5.78 (CHCHCH) and 6.15 (CHCHCH). In the ¹H NMR spectrum using CDCl₃, those protons appeared at 5.39 and 5.95, respectively. In the ¹³C NMR spectrum, the cyclopentadiene carbons appeared at 108 (CHCHCH) and 112.5 (CHCHCH). The pyridazine carbons appeared at 112.8 (CCN) and 151.5 (CCN). The carbon complexed to the manganese appeared at 222.5 (MnCO). Fortunately, our ¹³C NMR spectrum showed no signs of a carbonyl carbon, which is typically in the range of 170-175. This would indicate that we still had a fulvene and had not formed a pyridazine. In the IR spectrum, the C—N stretch showed up at 1607 cm⁻¹, the MnCO stretch appeared at 1941 and 2029

cm^{-1} , and the C—H stretch appeared at 3060 cm^{-1} . As with ^{13}C NMR, IR also showed no signs of carbonyl stretching, which can usually be found between 1500 and 1600 cm^{-1} .

Spectroscopy of $[\text{Re}(\text{CO})_3\text{-}\eta^5\text{-1,2-C}_5\text{H}_3(\text{CC}_4\text{H}_3\text{ON})(\text{CC}_4\text{H}_3\text{ON})\text{]}$ (4B)

The ^1H NMR spectrum showed a doublet at 7.59 (*CHCHCH*) and a triplet at 7.44 (*CHCHCH*) for the cyclopentadiene protons. The furoyl protons appeared in the $7.25\text{-}7.76$ range (*CHCHCHO*). The cyclopentadiene carbons appeared in the ^{13}C NMR spectrum at 108.5 (*CHCHCH*) and 110.0 (*CHCHCH*). The pyridazine carbons appeared at 117.5 (*CCN*) and 150.9 (*CCN*). The IR showed a peak at 1604 cm^{-1} for the C=N bond, peaks at 1890 and 2004 cm^{-1} for the ReCO bond, and 3056 cm^{-1} for the C—H bond. As with the spectroscopic data for **4A**, the spectroscopy data for this molecule showed no signs of a carbonyl carbon, indicating that we no longer had a fulvene.

Crystallization of $[M\{\eta^5\text{-1,2-C}_5\text{H}_3(\text{COC}_4\text{H}_3\text{O})_2\}(\text{CO})_3]$ (**3A** and **3B**)

Molecules **3A** and **3B** were able to be crystallized. Recrystallization of **3A** affords the diacyl complex as yellow-orange, block crystals (Fig. 4), while **3B** is red block crystals (Fig. 5). The diacyl complexes **3A** and **3B** both crystallize in a triclinic *P*-1 space group, and each have two molecules in the unit cell. The M–C Cp bonds are highly uniform for **3A**, with the deviations from the average length of 2.1457(16) Å no more than 0.012 Å. Re–C Cp bonds for **3B** also exhibit high uniformity with the deviations from the average length of 2.305(1) Å no more than 0.014 Å. X-ray analysis shows the two sets of carbonyls, the acyl C=O and the MnCO, having average bonds lengths of 1.224(2) Å and 1.1463(2) Å, respectively. In comparison, organic acyl and ReCO the average bonds lengths for **3B** proved similar (1.228(9) Å and 1.146(4) Å, respectively). In the solid state, the furoyl rings for **3A** and **3B** are highly asymmetric with respect to each other. The acyl portions for **3A** involving O1, C1–C4, and for **3B** involving O4, C12–15, are nearly planar with respect to their central Cp ring, with the C4–C5–C6–C7 (**3A**) and C9–C10–C11–C12 (**3B**) torsion angles at $-9.1(3)^\circ$ and at $-6.0(5)^\circ$, respectively. Conversely, the acyl moieties involving O4, C12–C15 (**3A**) and O1, C1–C4 (**3B**) are highly twisted out of plane of their Cp ring, with the C9–C10–C11–C12 and C4–C5–C6–C7 torsion angles at $-61.5(2)^\circ$ and at $108.1(3)^\circ$, respectively. ⁸

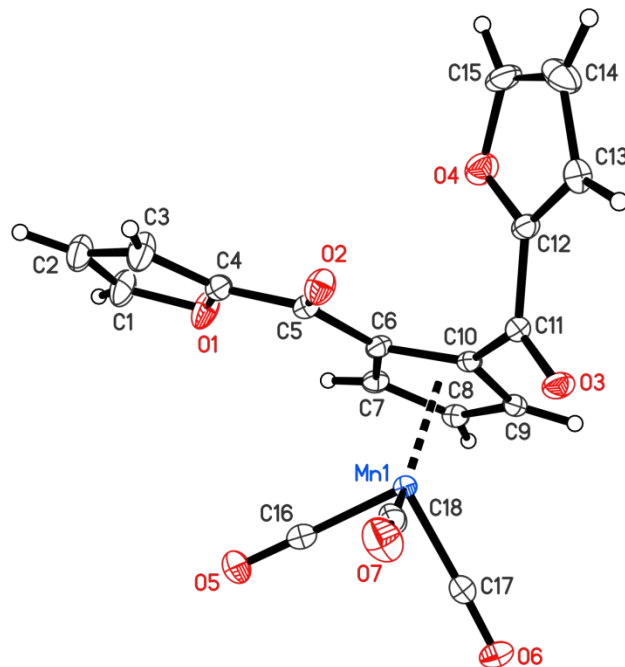


Figure 4: Crystal Structure of $[\text{Mn}\{\eta^5\text{-1,2-C}_5\text{H}_3(\text{COC}_4\text{H}_3\text{O})_2\}(\text{CO})_3]$ (**3A**)

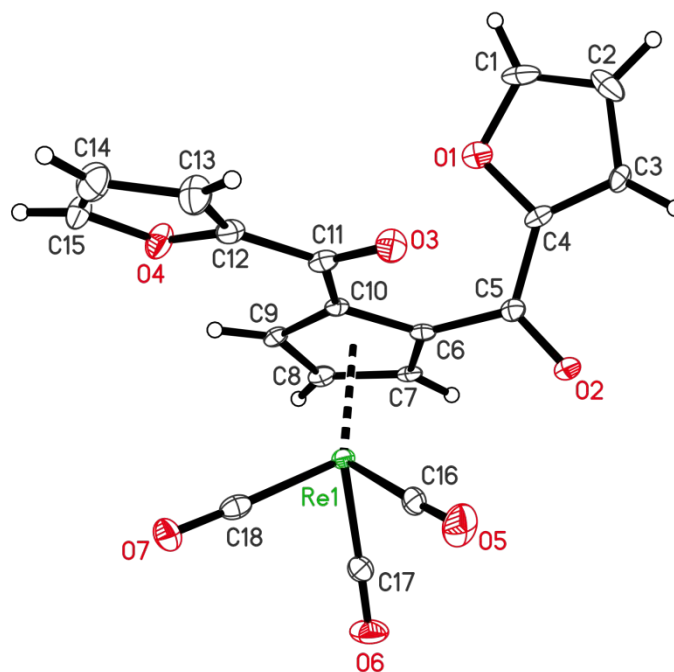


Figure 5: Crystal Structure of $[\text{Re}\{\eta^5\text{-1,2-C}_5\text{H}_3(\text{COC}_4\text{H}_3\text{O})_2\}(\text{CO})_3]$ (**3B**)

Table 1: Crystal data for 3A and 3B

Structure	3A	3B
Empirical formula	C ₁₈ H ₉ O ₇ Mn	C ₁₈ H ₉ O ₇ Re
Formula weight	392.19	523.45
Temperature	90.0(2) K	90.0(2) K
Wavelength	0.71073 Å	0.71073 Å
Crystal system, Space group	Triclinic, P-1	Triclinic, P-1
Unit cell dimensions	a = 7.6714(1) Å b = 7.7761(1) Å c = 14.7457(3) Å α = 97.1564(7) ^o β = 93.5724(7) ^o γ = 114.8305 ^o	a = 7.7072(1) Å b = 7.7210(1) Å c = 14.7324(3) Å α = 92.3941(7) ^o β = 96.3070(7) ^o γ = 112.9205 ^o
Volume	785.65(2) Å ³	799.15(2) Å ³
Z	2	2
Calculated density	1.658 Mg/m ³	2.175 Mg/m ³
Absorption coefficient	0.881 mm ⁻¹	7.643 mm ⁻¹
F(000)	396	496
Crystal size	0.18 x 0.15 x 0.12 mm	0.21 x 0.12 x 0.10 mm
θ range for data collection	1.40 to 27.46 ^o	1.40 to 25.00 ^o
Limiting indices	-9<=h<=9, -10<=k<=10, -19<=l<=19	-9<=h<=9, -9<=k<=9, -17<=l<=17
Reflections collected / unique	19312/3582 [R(int) = 0.0330]	16433/2814 [R(int) = 0.0360]
Absorption correction	Semi-empirical from equivalents	Semi-empirical from equivalents
Max. and min. transmission	0.903 and 0.859	0.515 and 0.335
Refinement method	Full-matrix least-squares on F ²	Full-matrix least-squares on F ²
Data/restraints/parameters	3582/0/235	2814/0/236
Goodness-of-fit on F ²	1.051	1.077
Final R indices [I>2 σ(I)]	R1 = 0.0298, wR2 = 0.0794	R1 = 0.0151, wR2 = 0.0336
R indices (all data)	R1 = 0.0340, wR2 = 0.0821	R1 = 0.0163, wR2 = 0.0341
Largest diff. peak and hole	0.547 and -0.389 e.Å ⁻³	1.393 and -0.698 e.Å ⁻³

CHAPTER 4

CONCLUSIONS

The formation of two new 1,4-difuryl pyridazine complexes **4A** and **4B** was accomplished in good yield by transmetallation of a 1,2-difuroylcyclopentadiene thallium salt **2** with $[\text{Mn}(\text{CO})_5\text{Br}]$ or $[\text{Re}(\text{CO})_5\text{Br}]$, followed by ring closure with hydrazine hydrate. X-ray crystallographic analysis of **3A** and **3B** confirmed the structures of diacyl precursors. IR and NMR data helped confirm the identity of the precursor molecules. A good portion of the product was lost when the product was extracted out of the solution. An example of this is the use of a silica plug to separate the product from other impurities. A significant amount of the product remained in the silica plug; however, we did not attempt to recover this product in order to avoid contamination with the impurities. Therefore, in a commercial setting the yield for this reaction could be raised significantly.

REFERENCES

1. Juster, N. J. Organic Semiconductors. *Journal of Chemical Education* **1963**, 40 (10), 547-555.
2. Bell, A. *A Modified Route to Cyclopenta(c)thiophenes via Grignard Reagents*; Masters Thesis; Western Kentucky University: Bowling Green, 2007.
3. OLED-Info. Sony XEL-1. oled-info.com (accessed November 5, 2010).
4. FGadgets. Samsung Foldable 3D OLED TV. fgadgets.com (accessed March 25, 2011).
5. Jacoby, M. The Power of Plastic: Polymer and organic molecule based solar cells show promise as low-cost power generators. *Chemical and Engineering News* **2010**, 12-16.
6. Gandini, A. Polymers from Renewable Resources: A Challenge for the Future of Macromolecular Materials. *Macromolecules* **2008**, 41 (9491).
7. Snyder, C. A.; Selegue, J. P.; Tice, N. C.; Wallace, C. E.; Blankenbuehler, M. T.; Parkin, S.; Allen, K. D. E.; Beck, R. T. J. Synthesis, Characterization, and Structure of Cyclopenta[c]thiophenes and Their Manganese Complexes. *Journal of American Chemical Society* **2005**, 127, 15010-15011.
8. Snyder, C. A.; Tice, N. C.; Maddox, J. B.; Emberton, E. D.; Vanover, E. S.; Hinson, D. F.; Jackson, D. C. Synthesis, Structure, and Electronic Study of Some Group VII Furoyl Substituted Complexes. *Journal of Organometallic Chemistry* **2011**, 696 (10), 2220-2222.
9. Bouffard, J.; Eaton, R. F.; Muller, P.; Swager, T. M. Iptycene-derived Pyridazines and Phthalazines. *Journal of Organic Chemistry* **2007**, 72 (26), 10166-10180.